

**Possible n/p-type conductivity of two-dimensional graphene oxide by boron and nitrogen doping: Evaluated via constrained excitation**

Dan Wang, Dong Han, Xian-Bin Li, Sheng-Yi Xie, Nian-Ke Chen, Wei Quan Tian, Shengbai Zhang, and Hong-Bo Sun

Citation: [Applied Physics Letters](#) **109**, 203113 (2016); doi: 10.1063/1.4967981

View online: <http://dx.doi.org/10.1063/1.4967981>

View Table of Contents: <http://scitation.aip.org/content/aip/journal/apl/109/20?ver=pdfcov>

Published by the [AIP Publishing](#)

---

**Articles you may be interested in**

[Enhancement of thermospin effect in ZGNRs via p-n co-doping on edge](#)

J. Appl. Phys. **120**, 135108 (2016); 10.1063/1.4964430

[Nitrogen-doped graphene films from simple photochemical doping for n-type field-effect transistors](#)

Appl. Phys. Lett. **106**, 013110 (2015); 10.1063/1.4905342

[Hybrid diodes based on n-type Ge and conductive polymer doped by graphene oxide sheets with and without reduction treatment](#)

J. Appl. Phys. **113**, 064502 (2013); 10.1063/1.4790889

[Electronic excitations in doped monolayer graphenes](#)

J. Appl. Phys. **106**, 113711 (2009); 10.1063/1.3266002

[Band structures, magnetic properties, and enhanced magnetoresistance in the high pressure phase of Gd and Y doped two-dimensional perovskite  \$Sr\_2CoO\_4\$  compounds](#)

Appl. Phys. Lett. **91**, 062501 (2007); 10.1063/1.2759273

---

The advertisement features a blue background with a glowing light effect and a molecular structure of blue spheres. On the left, there is a thumbnail image of an 'Applied Physics Reviews' journal cover showing a 3D diagram of a layered material. The main text 'NEW Special Topic Sections' is in large white font. Below it, 'NOW ONLINE' is in yellow, followed by the title 'Lithium Niobate Properties and Applications: Reviews of Emerging Trends' in white. The AIP Applied Physics Reviews logo is in the bottom right corner.

**NEW Special Topic Sections**

**NOW ONLINE**  
Lithium Niobate Properties and Applications:  
Reviews of Emerging Trends

**AIP** Applied Physics  
Reviews

## Possible *n/p*-type conductivity of two-dimensional graphene oxide by boron and nitrogen doping: Evaluated via constrained excitation

Dan Wang,<sup>1</sup> Dong Han,<sup>2</sup> Xian-Bin Li,<sup>1,a)</sup> Sheng-Yi Xie,<sup>1</sup> Nian-Ke Chen,<sup>1</sup> Wei Quan Tian,<sup>3</sup> Shengbai Zhang,<sup>4</sup> and Hong-Bo Sun<sup>1</sup>

<sup>1</sup>State Key Laboratory on Integrated Optoelectronics, College of Electronic Science and Engineering, Jilin University, Changchun 130012, China

<sup>2</sup>State Key Laboratory of Luminescence and Applications, Changchun Institute of Optics, Fine Mechanics and Physics, Chinese Academy of Sciences, Changchun 130033, China

<sup>3</sup>College of Chemistry and Chemical Engineering, Chongqing University, Huxi Campus, Chongqing 401331, China

<sup>4</sup>Department of Physics, Applied Physics, and Astronomy, Rensselaer Polytechnic Institute, Troy, New York 12180, USA

(Received 27 May 2016; accepted 5 November 2016; published online 16 November 2016)

As the first-principles calculations using the supercell approximation give widely scattered results in a two-dimensional charged system, making the evaluation of defect ionization energy difficult, here an alternative constrained excitation is applied to overcome this problem for defect analysis. As an example in graphene oxide with 50% oxygen coverage (according to the popular epoxy-chain-plus-hydroxyl-chain model), the structures, stabilities, and electronic properties of nitrogen and boron dopants are investigated. Generally, boron prefers to replace carbon in the  $sp^3$  region as an acceptor while nitrogen has a tendency to substitute the  $sp^2$  carbon close to the boundary between the  $sp^2$  region and the  $sp^3$  region as a donor. Their ionization energies are 0.24–0.42 eV for boron and 0.32–0.67 eV for nitrogen. However, a special case of nitrogen doped in the boundary- $sp^3$  carbon can change to be an acceptor with the assistance of its neighboring (epoxy) oxygen “Lift-off,” leading to the shallowest ionization energy of 0.12 eV and the best candidate for *p*-type conductivity. The present study offers the detailed pictures of boron and nitrogen defects in graphene oxide for the potential *n*- and *p*-type conductivity. *Published by AIP Publishing.*

[<http://dx.doi.org/10.1063/1.4967981>]

As silicon-based electronics is facing the challenge of maintaining the Moore’s Law through dimensional scaling,<sup>1</sup> our attention has been drawn to nanomaterials, such as graphene due to its fantastic properties.<sup>2–6</sup> However, the zero bandgap brings more challenges to the applications.<sup>1,4,7,8</sup> To open the bandgap, different methods have been proposed, such as quantum confinement effect,<sup>9–12</sup> chemical modification,<sup>13–16</sup> substrate,<sup>17,18</sup> and applying electric field.<sup>4,19</sup> Among them, graphene oxidation is much easier to achieve and control the energy gap.<sup>20</sup> Moreover, graphene oxide (GO) manifests many unique properties in electronic devices.<sup>21–23</sup> It would be expected that GO can be applied in semiconductor-based devices. To realize eventual industrialization, it is important to develop systematic understandings on the defect or doping properties of this material, in particular, the ability of defect to supply free carriers. However, charged defects in two-dimensional (2D) semiconductors have been very difficult to model theoretically when the traditional *Jellium* method is used due to the well-known energy divergence.<sup>24,25</sup>

In this letter, we adopt the constrained excitation (CE)<sup>26</sup> to explore the possible *n*-type or *p*-type conductivity by nitrogen or boron doping in GO (with 50% oxygen coverage), which is composed of the well-accepted epoxy chains and hydroxyl chains from many theoretical studies.<sup>27–29</sup> The present GO model has a direct bandgap of 1.80 eV. The

doping forms include substitution ( $N_C$ ,  $N_O$ ,  $B_C$ , and  $B_O$ ) and interstitial ( $N_i$  and  $B_i$ ). Generally, boron prefers to replace carbon in the  $sp^3$  region as an acceptor whereas nitrogen has a tendency to substitute the  $sp^2$  carbon close to the boundary between the  $sp^2$  region and the  $sp^3$  region as a donor. Their ionization energies are 0.24–0.42 eV for B and 0.32–0.67 eV for N. A special case named  $N_{C4}$  is nitrogen replacing a carbon, which is linked to an epoxy group. This nitrogen acts as an acceptor with the shallowest ionization energy of 0.12 eV above the valence band maximum (VBM). This phenomenon is attributed to the cooperating interaction between nitrogen and the original epoxy oxygen by the “Lift-off” mechanism. Compared to earlier studies of 2D graphene oxide, the present calculations provide an analysis of convergent ionization energy of boron/nitrogen defects for their potential *n*- or *p*-type conductivity.

The calculations are performed based on density functional theory (DFT),<sup>30</sup> with Perdew-Burke-Ernzerhof functional,<sup>31</sup> a kind of generalized gradient approximation, as implemented in Vienna Ab initio Simulation Package (VASP) codes.<sup>32</sup> There is no doubt that the electrostatic interactions can be better described by a better functional (such as hybrid functional) or many-body correction,<sup>33–35</sup> which will recover the band-gap-underestimation problem and then refresh the energies. But the methodology used in this work is applicable to any functional. In addition, time-dependent density functional theory is an important theory for excited states, especially for cluster or molecule systems

<sup>a)</sup> Author to whom correspondence should be addressed. Electronic address: [lixianbin@jlu.edu.cn](mailto:lixianbin@jlu.edu.cn)

in small size. We expect that it can be used to further improve the defect evaluation scheme in the near future. The GO model is constructed according to the theoretical works<sup>27–29,36</sup> and nuclear magnetic resonance experiments.<sup>37,38</sup> A graphene supercell with 96 carbon atoms is adopted as shown in Fig. 1(a). 24 hydroxyl groups and 12 epoxy groups (arranged in chains) are added on both sides of the graphene sheet with a total of 156 atoms [see Fig. 1(c)]. Along the  $z$  direction, a vacuum space of 13.6 angstrom is used to make sure that no interaction occurs between the model and its images. All atoms are allowed to relax until Hellman-Feynman force is less than 0.01 eV/Å. The effects of spin polarization were included. The cutoff energy of the plane wave is 450 eV, and the Monkhorst-Pack  $k$ -point mesh grid is  $2 \times 1 \times 1$  for the Brillouin zone integration.

To determine the electron ionization ability of impurities, the formation energies and transition levels of defects are calculated. The formation energy of a dopant in host, which determines the possibility of its existence, can be expressed as<sup>39–41</sup>

$$\Delta E_f^{(q,d)} = \Delta E^{(q,d)} + n_d \mu_d + q \varepsilon_F, \quad (1)$$

where

$$\Delta E^{(q,d)} = E^{(q,d)}(\text{host} + d) - E(\text{host}) + n_d \mu_d(\text{solid}) + q \varepsilon_{VBM}. \quad (2)$$

Here,  $E^{(q,d)}(\text{host} + d)$  is the total energy of the supercell containing a defect  $d$  with charge  $q$ , and  $E(\text{host})$  is the total energy of the pristine supercell.  $n_d$  is the number of atoms being exchanged during defect formation. For example,  $n_C = 1$  and  $n_N = -1$  for the creation of nitrogen substitution for carbon.  $\mu_d$  is the chemical potential of the reservoir referenced to its most stable element form, such as  $\mu_d(\text{solid})$ , the chemical potential of  $d$  at the solid form.  $\varepsilon_F$  is the Fermi energy measured from the VBM denoted by  $\varepsilon_{VBM}$ . The Fermi energy at which two different charge states ( $q$  and  $q'$ ) of

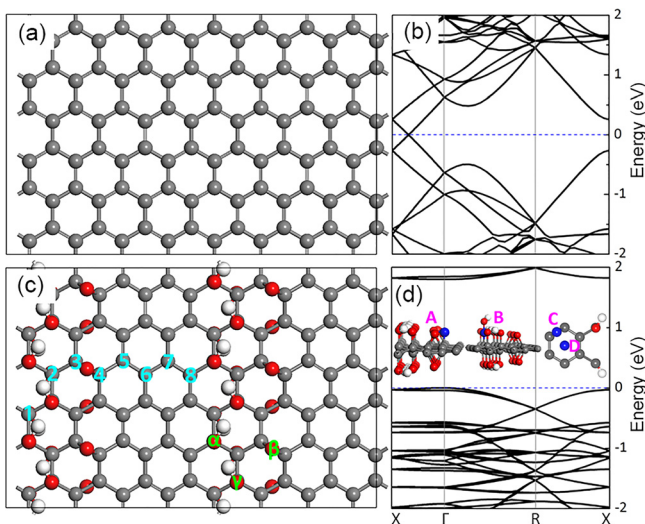


FIG. 1. (a) and (b) The geometry and band structure of graphene. (c) and (d) The geometry and band structure of the GO with 50% oxygen coverage. Numbers and Greek letters indicate the different substitution doping sites. Interstitial forms are shown in the inset in (d). Grey, red, white, and blue balls represent the carbon, oxygen, hydrogen, and dopant atoms, respectively.

the same defect  $d$  has the same formation energy  $\Delta E_f^{(q,d)} = \Delta E_f^{(q',d)}$  defines the defect transition level  $\varepsilon(q/q')$ . Hence

$$\varepsilon(q/q') = [\Delta E^{(q,d)} - \Delta E^{(q',d)}] / (q' - q). \quad (3)$$

For charged states, the periodic boundary condition in the first-principles calculation can introduce artificial long-range Coulomb interactions between the defect and its images. As a consequence, it introduces divergence in the total energy. Usually, a homogeneous counter charge (the so-called *Jellium* background) is introduced to neutralize the cell.<sup>42</sup> Such a computational scheme for charged defects has been widely used for three-dimension (3D) solids. However, the *Jellium* charges extend to vacuum in 2D systems [see Fig. 2(a)] resulting in strong Coulomb interactions with charged defects. This Coulomb energy diverges with the vacuum dimension, so the results for charged defects with such a way can scatter widely as elucidated.<sup>24</sup> As

$$\Delta E_f^{(q,d)} = \Delta E_f^{(0,d)} + q[\varepsilon_F - \varepsilon(q/0)], \quad (4)$$

where the formation energy of neutral defect  $\Delta E_f^{(0,d)}$  can be readily calculated without any errors, so, finding  $\Delta E_f^{(q,d)}$  is equivalent to finding  $\varepsilon(q/0)$  and the two have the same divergence in 2D systems. The ionization energy here means the energy required to ionize electrons from the impurity level into the conduction band minimum (CBM) for the donor-type defect or holes from the impurity level into the VBM for the acceptor-type defect. This is different from the formal definition of ionization energy, i.e., the energy to remove an electron from the system. The CE is applied here to avoid divergence. In that way, the ionized carrier is removed from the impurity level and is also constrained at the corresponding band edge (take donor as an example, see Fig. 2(b)).<sup>26</sup> The system is kept in the neutral state through all calculations, and thus the ionized carrier just localizes

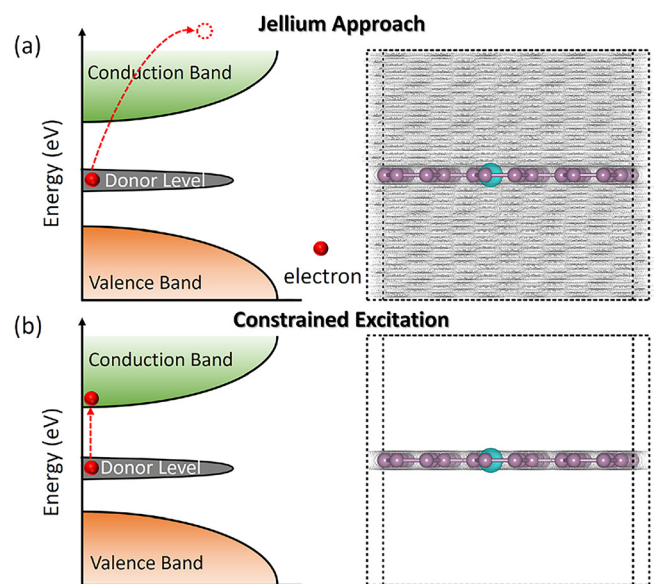


FIG. 2. Schematic diagram of ionized-electron distribution in reciprocal (left) and real space (right) in (a) *Jellium* method and (b) Constrained Excitation method. The blue ball on the right represents the defect position in a two-dimensional sheet and the shadow areas display the ionized carrier distribution.

around the 2D sheet. Finally, convergent ionization energy can be obtained by the energy difference between the ground state and excited state. Then, the charged formation energy can be derived from Equation (4). In CE, only the Gamma-point in the Brillouin zone is used, and the spin of the system is also kept. The ionization energies obtained by the CE method here are different from those obtained by the extrapolation method of Ref. 24. The difference comes from the Coulomb binding between the ionized electrons/holes and charged defects in the 2D system.<sup>43</sup> However, such binding can be weakened by high-dielectric environments (e. g., from substrate) with enhanced screening.<sup>43–45</sup> Therefore, the ionization energies given here are of significance in exploring the defect pictures of nitrogen-/boron-doped graphene oxide.

The detailed chemical structure of GO remains unclear in experimental synthesis. It is generally accepted that a significant amount of carbon atoms of GO remains in the  $sp^2$  form along with a part of  $sp^3$  carbon atoms bonded to either epoxy (i.e., bridge oxygen) or hydroxyl (i.e., -OH) groups.<sup>37,38</sup> The arrangement of these functional groups has been identified by a lot of first-principles calculations from the energetic point of view.<sup>27–29,36</sup> Three rules can be summarized to choose the GO model. First, hydroxyl groups tend to form chains to maximize the interaction via hydrogen bonds, and the epoxy groups are also grouped next to the hydroxyl chain. Second, armchair chains are always more stable than the zigzag chains. Third, the functional groups prefer to aggregate on both sides of the carbon sheet to maintain its flatness without vertical distortion.

According to the above rules, as shown in Fig. 1(c), we construct a model of GO with 50% coverage (number of  $sp^3$ -carbon/total number of carbon atoms  $\times$  100%) on the basis of the pure  $sp^2$  carbon sheet [Fig. 1(a)]. 24 hydroxyl groups and 12 epoxy groups constitute its chemical formulas as  $C_{96}O_{12}(OH)_{24}$ . In Figs. 1(b) and 1(d), we show the band dispersions for graphene and GO, respectively. The GO has a direct band gap of 1.80 eV at the Gamma point, which is the same order of magnitude with other 2D semiconductors in calculations. Three kinds of doping sites for nitrogen and boron according to the different chemical environment are considered in Fig. 1(c). For nitrogen/boron replacing carbon ( $N_C$  and  $B_C$ ), 1–2, 3–4, and 5–8 indicate the substitutions for the hydroxyl-functioned carbon, the substitutions for the epoxy-functioned carbon, and the substitutions for the bare  $sp^2$  carbon, respectively. For nitrogen/boron replacing oxygen ( $N_O$  and  $B_O$ ),  $\beta$  indicates the substitution for epoxy oxygen while  $\alpha$  and  $\gamma$  indicate substitution for hydroxyl oxygen. For nitrogen/boron interstitial ( $N_i$  and  $B_i$ ), A/B ( $N_{iA}$ ,  $N_{iB}$ ,  $B_{iA}$ , and  $B_{iB}$ ) are the sites between oxygen and its connected carbon; C ( $N_{iC}$  and  $B_{iC}$ ) are the bridge sites between two connected bare carbon; and D ( $N_{iD}$ ,  $B_{iD}$ ) are the sites above the center of a carbon hexagon, respectively. The optimized local configurations of nitrogen-related ( $N_C$ ,  $N_O$ , and  $N_i$ ) and boron-related defects ( $B_C$ ,  $B_O$ , and  $B_i$ ) are shown in Figs. S1 and S2 of the supplementary material.

To evaluate the stability, we calculated the neutral formation energies of all the cases as shown in Table SI. For nitrogen-related defects,  $N_C$  (1.04–1.55 eV) generally have lower neutral formation energies than  $N_O$  and  $N_i$  (3.06–4.48 eV) except  $N_{C2}$  (3.69 eV) and  $N_{C3}$  (2.88 eV), in

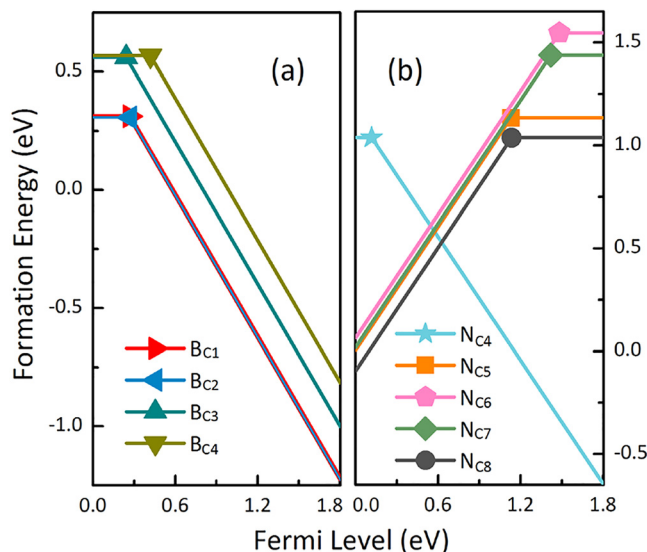


FIG. 3. Calculated formation energies as a function of Fermi level for the (a) boron-related defects and (b) nitrogen-related defects. The Fermi level varies from 0 at VBM to 1.80 eV at CBM according to the calculated bandgap of the GO.

which the fourfold coordination of nitrogen increases the energy. In addition, the formation energies of  $N_{C5}$  and  $N_{C8}$  are 1.14 eV and 1.04 eV, which are lower than 1.55 eV and 1.44 eV of  $N_{C6}$  and  $N_{C7}$ . These results reveal that nitrogen atom favors substituting the  $sp^2$  or bare carbon atoms close to the boundary between the  $sp^2$  region and the  $sp^3$  region. Concerning boron, substitution for the  $sp^3$  carbon ( $B_{C1}$ – $B_{C4}$ ) is more energetically favorable than substitution for the  $sp^2$  carbon atom ( $B_{C5}$ – $B_{C8}$ ).

Except for the defects with the reaction to produce the  $H_2O$  molecule ( $N_{C1}$ ,  $B_{O\alpha}$  and  $B_{iB}$ ), the relatively stable configurations (i.e.,  $N_{C4}$ ,  $N_{C5}$ – $N_{C8}$ , and  $B_{C1}$ – $B_{C4}$ ) are chosen to analyze the doping properties. The formation energies of these cases, as a function of  $\epsilon_F$ , are shown in Fig. 3, and the corresponding transition levels are displayed in Fig. 4. As nitrogen/boron has one more or less electron than carbon, nitrogen/boron substitution usually induces a spin-occupied/spin-unoccupied energy level in the bandgap. The occupied level in  $N_{C5}$ – $N_{C8}$  (as a representative, see  $N_{C5}$  in Fig. S3(a)) is close to the CBM, which means the larger possibility to donate an electron as a donor. By the same token, the

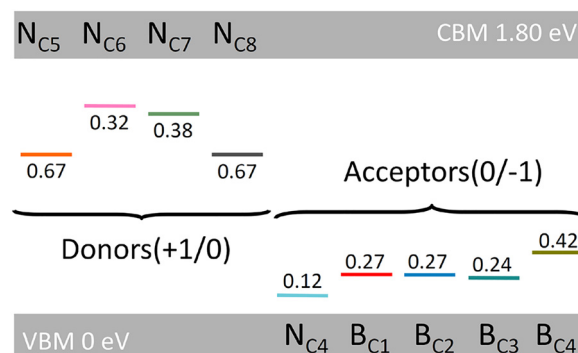


FIG. 4. The calculated transition levels (ionization energy) for the energetically favorable defects by the CE method. The values are shown with respect to VBM for acceptors and CBM for donors.

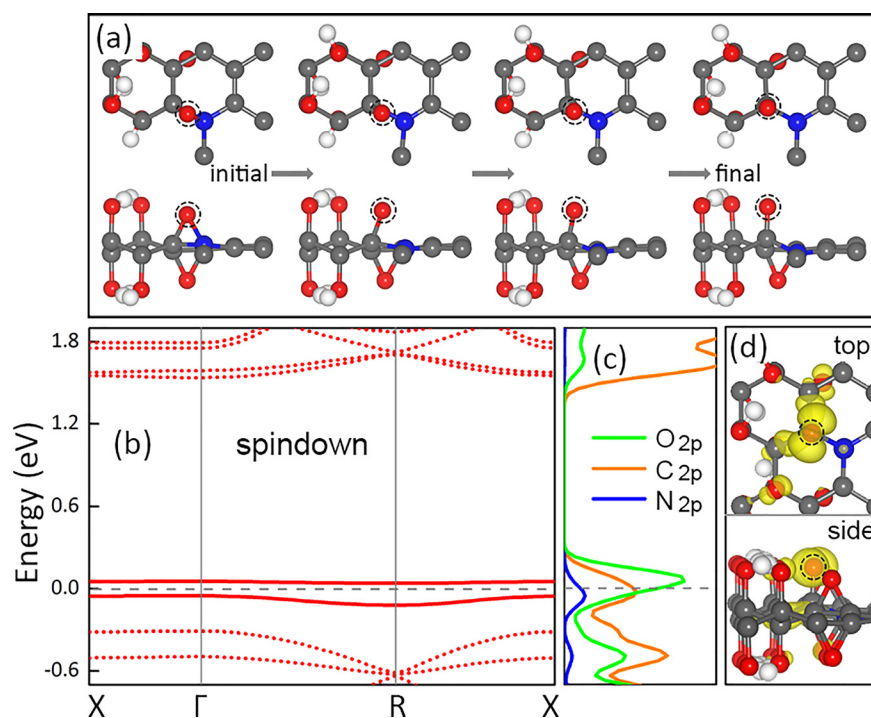


FIG. 5. (a) The local structure evolution of the “Lift-off” mechanism for  $N_{C4}$  during relaxation. (b) The spin-down band structure. Solid lines represent the impurity levels of  $N_{C4}$  within the bandgap. (c) The partial density of states and (d) the charge density distribution of the unoccupied acceptor level (red solid line above Fermi level in (b)). The grey, red, white, and blue balls represent carbon, oxygen, hydrogen, and nitrogen atoms, respectively. The isosurface of spin electron density is  $0.004 e/a_0^3$ , where  $a_0$  is the Bohr radius. The Fermi level is at 0 eV.

unoccupied level in  $B_{C1}$ - $B_{C4}$  (see  $B_{C1}$  in Fig. S3(b) for an example) is likely to accept an electron from the VBM as an acceptor. For  $N_{C4}$ , the unoccupied level is close to the VBM and the two occupied levels are far away from the CBM as shown in Fig. S3(c). Thus,  $N_{C4}$  is more favorable to be an acceptor. In the light of the analysis above, we calculate the transition level of (+1/0) for  $N_{C5}$ - $N_{C8}$  and (0/-1) for  $B_{C1}$ - $B_{C4}$ ,  $N_{C4}$ . The acceptor transition levels of  $B_{C1}$ ,  $B_{C2}$ ,  $B_{C3}$ , and  $B_{C4}$  are 0.27 eV, 0.27 eV, 0.24 eV, and 0.42 eV above the VBM, respectively. For nitrogen, the donor transition levels of  $N_{C6}$  and  $N_{C7}$ , being 0.32 eV and 0.38 eV below the CBM, are shallower than those of  $N_{C5}$  and  $N_{C8}$ , being 0.67 eV and 0.67 eV below the CBM. This can be understood by noting that the CBM is mainly derived from the  $p$  orbitals of bare carbon, see Fig. S4. Moreover, for the  $sp^2$  carbon, the closer to the  $sp^3$  carbon, the greater contribution to the CBM. Thus,  $N_{C6}$  and  $N_{C7}$  perform smaller perturbation on the CBM than  $N_{C5}$  and  $N_{C8}$  do. In addition, the relative deepness of the ionization energies of  $N_{C5}$ - $N_{C8}$  matches the cases of defect levels in band structures, as shown in Fig. S5. The best candidates for  $n$ -type doping by nitrogen and  $p$ -type doping by boron are predicted to be  $N_{C6}$  (0.32 eV below CBM) and  $B_{C3}$  (0.24 eV above VBM), respectively. However, according to the conventional standard for carrier ionization (ionization energy  $< 0.2$  eV), such two kinds of defects hardly contribute enough carriers for electronic devices.

Unexpectedly, another case of nitrogen of  $N_{C4}$  induces a much shallower acceptor level, being 0.12 eV above the VBM. The unusual  $p$ -type doping behavior can be understood as follows. In Fig. 5, first, the initial nitrogen replaces the carbon connecting to epoxy. Then, nitrogen instantly breaks the bond with the epoxy oxygen (here named it “Lift-off” mechanism) and just maintains three bonds with the three adjacent carbon, see Fig. 5(a). Different from  $N_{C5}$ - $N_{C8}$ , the unoccupied acceptor level in  $N_{C4}$  [see the red solid line above the Fermi level in Fig. 5(b)], above but close to the VBM, is actually

derived from the  $p$  orbit of the “Lift-off” oxygen according to electronic distribution in Fig. 5. This can be understood that nitrogen favors to form three coordination plus a lone pair due to its  $s^2p^3$  configuration, resulting in no contribution to the unoccupied acceptor level. However, the original epoxy oxygen just leaves a single bond with the other carbon and also has an unpaired  $p$  electron. This unpaired  $p$  electron favors to capture another electron to meet the octet rule for the oxygen and thus acts as the acceptor. The strong electronegativity of oxygen further makes the acceptor shallow. Here, we stress that the formation energy of  $N_{C4}$  is still relatively small with 1.04 eV. This reveals that the existence of epoxy benefits the desired  $p$ -type conductivity in nitrogen-doping GO.

In summary, the doping properties of nitrogen and boron in graphene oxide with a 50% oxygen coverage model have been systematically studied with first-principles calculations. Due to the weak screening of low-dimensional systems, the conventional calculations of charged defects using supercell approximation give the divergent energy. Here, the convergent transition energies are efficiently evaluated by the constrained excitation. Generally, boron prefers to replace carbon in the  $sp^3$  region as an acceptor while nitrogen has a tendency to substitute the  $sp^2$  carbon close to the boundary between the  $sp^2$  region and the  $sp^3$  region as the donor. However, a special case of nitrogen can change to be an effective acceptor through the “Lift-off” motion of its neighboring (epoxy) oxygen, which results in the shallowest ionization energy of 0.12 eV for  $p$ -type conductivity. The present study offers a microscopic picture of defect doping behavior in GO for future electronic devices applications.

See [supplementary material](#) for atomic geometries, band structures, and formation energies of the nitrogen-/boron-related defects; and the charge density distribution of conduction band minimum and valence band maximum of graphene oxide.

The work was supported by the National Natural Science Foundation of China (11374119, 11504368, 61590930, and 91423102) and 973 Program (2014CB921303). W.Q.T. acknowledges the support from the Open Project of State Key Laboratory of Supramolecular Structure and Materials (JLU) (No. SKLSSM201620). Also, we acknowledge the High Performance Computing Center (HPCC) at Jilin University for calculation resources.

- <sup>1</sup>K. Kim, J.-Y. Choi, T. Kim, S.-H. Cho, and H.-J. Chung, *Nature* **479**, 338 (2011).
- <sup>2</sup>K. S. Novoselov, D. Jiang, F. Schedin, T. J. Booth, V. V. Khotkevich, S. V. Morozov, and A. K. Geim, *Proc. Natl. Acad. Sci. U. S. A.* **102**, 10451 (2005).
- <sup>3</sup>A. K. Geim and K. S. Novoselov, *Nat. Mater.* **6**, 183 (2007).
- <sup>4</sup>F. Schwierz, *Nat. Nanotechnol.* **5**, 487 (2010).
- <sup>5</sup>W. Streck, B. Cichy, L. Radosinski, P. Gluchowski, L. Marciniak, M. Lukaszewicz, and D. Hreniak, *Light: Sci. Appl.* **4**, e237 (2015).
- <sup>6</sup>J.-H. Chen, B.-C. Zheng, G.-H. Shao, S.-J. Ge, F. Xu, and Y.-Q. Lu, *Light: Sci. Appl.* **4**, e360 (2015).
- <sup>7</sup>K. S. Novoselov, A. K. Geim, S. V. Morozov, D. Jiang, Y. Zhang, S. V. Dubonos, I. V. Grigorieva, and A. A. Firsov, *Science* **306**, 666 (2004).
- <sup>8</sup>F. Xia, D. B. Farmer, Y. M. Lin, and P. Avouris, *Nano Lett.* **10**, 715 (2010).
- <sup>9</sup>Y.-W. Son, M. L. Cohen, and S. G. Louie, *Phys. Rev. Lett.* **97**, 216803 (2006).
- <sup>10</sup>M. Y. Han, B. Özyilmaz, Y. B. Zhang, and P. Kim, *Phys. Rev. Lett.* **98**, 206805 (2007).
- <sup>11</sup>L. A. Ponomarenko, F. Schedin, M. I. Katsnelson, R. Yang, E. W. Hill, K. S. Novoselov, and A. K. Geim, *Science* **320**, 356 (2008).
- <sup>12</sup>L. Jiao, L. Zhang, X. Wang, G. Diankov, and H. Dai, *Nature* **458**, 877 (2009).
- <sup>13</sup>S. Y. Zhou, D. A. Siegel, A. V. Fedorov, and A. Lanzara, *Phys. Rev. Lett.* **101**, 086402 (2008).
- <sup>14</sup>D. W. Boukhvalov and M. I. Katsnelson, *J. Phys.: Condens. Matter* **21**, 344205 (2009).
- <sup>15</sup>D. C. Elias, R. R. Nair, T. M. G. Mohiuddin, S. V. Morozov, P. Blake, M. P. Halsall, A. C. Ferrari, D. W. Boukhvalov, M. I. Katsnelson, A. K. Geim, and K. S. Novoselov, *Science* **323**, 610 (2009).
- <sup>16</sup>G. Eda, C. Mattevi, H. Yamaguchi, H. Kim, and M. Chhowalla, *J. Phys. Chem. C* **113**, 15768 (2009).
- <sup>17</sup>G. Giovannetti, P. A. Khomyakov, G. Brocks, P. J. Kelly, and J. van den Brink, *Phys. Rev. B* **76**, 073103 (2007).
- <sup>18</sup>S. Kim, J. Ihm, H. J. Choi, and Y. W. Son, *Phys. Rev. Lett.* **100**, 176802 (2008).
- <sup>19</sup>E. V. Castro, K. S. Novoselov, S. V. Morozov, N. M. Peres, J. M. dos Santos, J. Nilsson, F. Guinea, A. K. Geim, and A. H. Neto, *Phys. Rev. Lett.* **99**, 216802 (2007).
- <sup>20</sup>K.-C. Zhang, Y.-F. Li, Y. Liu, and Y. Zhu, *Carbon* **102**, 39 (2016).
- <sup>21</sup>C. Gómez-Navarro, R. T. Weitz, A. M. Bittner, M. Scolari, A. Mews, M. Burghard, and K. Kern, *Nano Lett.* **7**, 3499 (2007).
- <sup>22</sup>G. Eda, G. Fanchini, and M. Chhowalla, *Nat. Nanotechnol.* **3**, 270 (2008).
- <sup>23</sup>X. Wu, M. Sprinkle, X. Li, F. Ming, C. Berger, and W. A. de Heer, *Phys. Rev. Lett.* **101**, 026801 (2008).
- <sup>24</sup>D. Wang, D. Han, X.-B. Li, S.-Y. Xie, N.-K. Chen, W. Q. Tian, D. West, H.-B. Sun, and S. B. Zhang, *Phys. Rev. Lett.* **114**, 196801 (2015).
- <sup>25</sup>H.-P. Komsa and A. Pasquarello, *Phys. Rev. Lett.* **110**, 095505 (2013).
- <sup>26</sup>P. Tangney and S. Fahy, *Phys. Rev. B* **65**, 054302 (2002).
- <sup>27</sup>J.-A. Yan, L. Xian, and M. Chou, *Phys. Rev. Lett.* **103**, 086802 (2009).
- <sup>28</sup>L. Wang, Y. Y. Sun, K. Lee, D. West, Z. F. Chen, J. J. Zhao, and S. B. Zhang, *Phys. Rev. B* **82**, 161406 (2010).
- <sup>29</sup>J.-A. Yan and M. Y. Chou, *Phys. Rev. B* **82**, 125403 (2010).
- <sup>30</sup>P. Hohenberg and W. Kohn, *Phys. Rev.* **136**, B864 (1964).
- <sup>31</sup>J. P. Perdew, K. Burke, and M. Ernzerhof, *Phys. Rev. Lett.* **77**, 3865 (1996).
- <sup>32</sup>G. Kresse and J. Furthmüller, *Phys. Rev. B* **54**, 11169 (1996).
- <sup>33</sup>G. Luo, X. Qian, H. Liu, R. Qin, J. Zhou, L. Li, Z. Gao, E. Wang, W.-N. Mei, J. Lu, Y. Li, and S. Nagase, *Phys. Rev. B* **84**, 075439 (2011).
- <sup>34</sup>S. Pari, A. Cuéllar, and B. M. Wong, *J. Phys. Chem. C* **120**, 18871 (2016).
- <sup>35</sup>D. West, Y. Y. Sun, and S. B. Zhang, *Appl. Phys. Lett.* **101**, 082105 (2012).
- <sup>36</sup>D. W. Boukhvalov and M. I. Katsnelson, *J. Am. Chem. Soc.* **130**, 10697 (2008).
- <sup>37</sup>W. Cai, R. D. Piner, F. J. Stadermann, S. Park, M. A. Shaibat, Y. Ishii, D. Yang, A. Velamakanni, S. J. An, M. Stoller, J. An, D. Chen, and R. S. Ruoff, *Science* **321**, 1815 (2008).
- <sup>38</sup>W. Gao, L. B. Alemany, L. Ci, and P. M. Ajayan, *Nat. Chem.* **1**, 403 (2009).
- <sup>39</sup>S. B. Zhang and J. E. Northrup, *Phys. Rev. Lett.* **67**, 2339 (1991).
- <sup>40</sup>D. Han, D. West, X.-B. Li, S.-Y. Xie, H.-B. Sun, and S. B. Zhang, *Phys. Rev. B* **82**, 155132 (2010).
- <sup>41</sup>D. Han, Y. Y. Sun, J. Bang, Y. Y. Zhang, H.-B. Sun, X.-B. Li, and S. B. Zhang, *Phys. Rev. B* **87**, 155206 (2013).
- <sup>42</sup>C. G. Van de Walle, P. J. H. Denteneer, Y. Bar-Yam, and S. T. Pantelides, *Phys. Rev. B* **39**, 10791 (1989).
- <sup>43</sup>D. Wang, D. Han, X.-B. Li, N.-K. Chen, S.-Y. Xie, D. West, W. Q. Tian, S. B. Zhang, and H.-B. Sun, "Low-Energy Excitation of Defect State in Two-Dimensional Semiconductors and its Implication to Carrier Transport" (unpublished).
- <sup>44</sup>B. Radisavljevic, A. Radenovic, J. Brivio, V. Giacometti, and A. Kis, *Nat. Nanotechnol.* **6**, 147 (2011).
- <sup>45</sup>J.-Y. Noh, H. Kim, M. Park, and Y.-S. Kim, *Phys. Rev. B* **92**, 115431 (2015).